Int. J. Electrochem. Sci., 17 **(2022)** Article Number: 220941, doi: 10.20964/2022.09.47

International Journal of
ELECTROCHEMICAL
SCIENCE
www.electrochemsci.org

Electrochemical Sensor Based on Graphene Oxide Nanocomposite for Determination of Dexamethasone in Pharmaceutical Samples

Jingtian Xu[*]

School of Electronic Engineering, Xi'an Shiyou University, 710065, Xi'an, Shaanxi, China
[*]E-mail: jtxu@xsyu.edu.cn

Received: 7 June 2022 / *Accepted:* 5 July 2022 / *Published:* 7 August 2022

The current research is focused on the electrochemical determination of dexamethasone (DEX) in pharmaceutical samples and the production of ZnO and graphene oxide nanocomposite modified screen-printed electrodes (ZnO@GO/SPE) utilizing a simple chemical technique. According to XRD and SEM investigations, the hexagonal crystal structure of GO nanosheets of hexagonal wurtzite ZnO nanorods was successfully combined into a sandwich-like ZnO@GO nanocomposite structure. ZnO@GO/SPE is a selective, more stable, and sensitive DEX sensor than ZnO/SPE and GO/SPE, according to electrochemical tests employing DPV and amperometry techniques. Because of its good stability and large accessible specific surface area for analyte adsorption from electrolyte, the ZnO@GO nanocomposite had a linear range of 10 to 200 μM, sensitivity of 0.20211μA/μM, and a limit of detection of 12 nM, which showed comparable or even better sensing performance than other reported DEX sensors in the literature. This improved the charge transfer between the electrode and the analyte of ZnO@GO nanocomposite. e practical capability of the ZnO@GO/SPE was tested for determining DEX level in dexamethasone injection, and the results showed that the recovery (96.50% to 99.16%) and RSD (3.33% to 4.35%) values were appropriate for practical analyses in clinical and pharmaceutical samples, indicating appropriate validity and accuracy.

Keywords: Graphene Oxide nanocomposite; ZnO nanorods; Dexamethasone; Pharmaceutical Samples; Amperometry

1. INTRODUCTION

Dexamethasone (DEX, $C_{22}H_{29}FO_5$), also known as Decadron and Dexasone, is a glucocorticoid medication used to treat rheumatoid arthritis, severe allergies, asthma, chronic obstructive pulmonary disease, croup, brain swelling, a variety of endocrine diseases, hematologic disorders, superior vena cava syndrome, and tuberculosis when combined with antibiotics [1, 2]. DEX is a corticosteroid that helps to alleviate swelling, redness, itching, and allergic reactions by acting on the immune system [3].

Corticosteroids bind to the glucocorticoid receptor, which inhibits pro-inflammatory impulses while increasing anti-inflammatory ones [4, 5]. DEX's action lasts a different amount of time depending on the route. Patients may require doses that are multiples of what the body generates naturally, so corticosteroids have a broad therapeutic window [6, 7].

Long-term use of DEX might cause eye disorders like cataracts and glaucoma. Optic nerve damage, as well as fungal or viral eye infections, are possible side effects of the medicine [8, 9]. Due to adrenal insufficiency, DEX can cause physical dependence and steroid withdrawal [10, 11]. Corticosteroids can cause the adrenal glands, which are responsible for manufacturing natural corticosteroids, to malfunction [12, 13].

Furthermore, DEX is well-known in the world of sport as a low-cost anti-inflammatory steroid that has been used by athletes for years to speed up their recovery from injuries and infections [14, 15]. Corticosteroids have a faster onset of performance advantages. Injections of corticosteroids into the muscles or oral corticosteroids can help with the discomfort and inflammation that comes with high-intensity exercise [16, 17]. The epimeric corticosteroid DEX is particularly effective and long-acting in equestrian activities such as cycling and horse racing, and it is often abused [18, 19]. To prevent its misuse related to euphoria and pain suppression, the use of DEX is controlled and restricted by some sports federations [20, 21]. According to the World Anti-Doping Agency, these modes of administration result in a considerable amount of glucocorticoids circulating in the blood, which could improve performance or harm health [22-24].

Determination of DEX using capillary electrophoresis [25], spectrophotometry [26], high performance liquid chromatography [27], gas chromatography with negative chemical ionization mass spectrometry [28], radioimmunoassay [29], UV-spectroscopy [30] and electrochemistry [20, 31-36] has thus been the subject of numerous studies. Electrochemical sensors offer the most potential to increase accuracy, sensitivity, linear range, and detection limit among these approaches [36-38] by modifying the electrode surface using nanostructures and nanocomposites. As a result, the current research is focused on the fabrication of ZnO@GO nanocomposite for the detection of DEX in pharmaceutical samples.

2. MATERIALS AND METHOD

2.1. Synthesis of ZnO@GO nanocomposite

The ZnO@GO nanocomposite was made via a straightforward chemical method [39]: Ultrasonically dispersed 20 mg GO nanosheets (99%, Globalchemical Factory Co., Ltd., China) in 20 mL dimethylformamide (DMF, 99%, Shandong Near Chemical Co.,Ltd., China). After 5 minutes of ultrasonication, 80 ml of 20 mM zinc acetate dihydrate (99.999%, Sigma-Aldrich) was stirred vigorously for 10 minutes with the GO suspension. The suspension was then heated for 6 hours at 85 °C to obtain a grayish-white powder as ZnO@GO nanocomposite. After washing the powder three times with ethanol (99%, Shanghai Zhongrong Technology Co., Ltd., China), it was centrifuged for five minutes at 1500 rpm. The items were placed in the oven and dried for 3 hours at 55°C. The same

process was used to make ZnO nanorods without the use of GO nanosheets. The modified screen-printed electrode (SPE) was made by ultrasonically preparing a 1g/L suspension of ZnO@GO nanocomposite or ZnO or GO in deionized water. On the SPE, the dispersed suspension was cast and cured at room temperature.

2.2. Characterization

The electrochemical workstation potentiostat galvanostat (TOB-CS-300, Xiamen Tob New Energy Technology Co., Ltd., China) equipped with a cell containing a three-electrode platinum plate, Ag/AgCl, and modified SPE as the counter, reference, and working electrodes, respectively, was used to conduct DPV and amperometry experiments. Electrochemical tests were carried out using 0.1M PBS (pH 7.0) as the electrolyte, which was made from an equal volume ratio of 0.1M NaH2PO4 (99%, Jiangsu Kolod Food Ingredient Co., Ltd., China) and 0.1M Na2HPO4 (99%, Jiangsu Kolod Food Ingredient Co., Ltd., China). The X-ray diffraction (XRD) patterns of samples were obtained using a Bruker D8 127 diffraction analyzer. Scanning electron microscopy (SEM; HILIPS XL30/TMP, the Netherlands) was used to examine the morphology of produced nanostructures.

2.3. Actual samples preparation

1 mL of dexamethasone 3.3 mg/mL injection (Hameln Pharma Ltd., Brockworth, England) was mixed with 199 mL of 0.1 M PBS to generate the pharmaceutical real samples of 0.0165 mg/mL (42 M) DEX (pH 7.0). The amperometric measurement at -0.93 V was used for electrochemical analysis, and the standard addition method was used for analytical examinations of actual materials.

3. RESULTS AND DISCUSSION

3.1. XRD and SEM studies

XRD patterns of powders of GO, ZnO, and ZnO@GO nanocomposite are shown in Figure 1. The XRD pattern of GO reveals a distinctive peak at 26.42°, which is related to a basal reflection (002) caused by oxygen carrying groups on the GO-surface and the hexagonal crystal structure of GO nanosheets [40-42]. The peaks at 31.77°, 34.39°, 36.19°, 47.39°, 56.658°, 62.88°, 65.5°, 67.98°, and 69.08° in the diffractogram of ZnO and ZnO@GO nanocomposite are allocated to (100), (002), (101), (102), (110), (103), (200), (112), and (201) reflection planes, respectively, indicating that hexagonal (JCPDS Card No. 36-1451) [43, 44]. The combining of GO nanosheets of ZnO nanorods into ZnO@GO nanocomposite is demonstrated by the additional shoulder of GO in the XRD pattern of ZnO@GO nanocomposite.

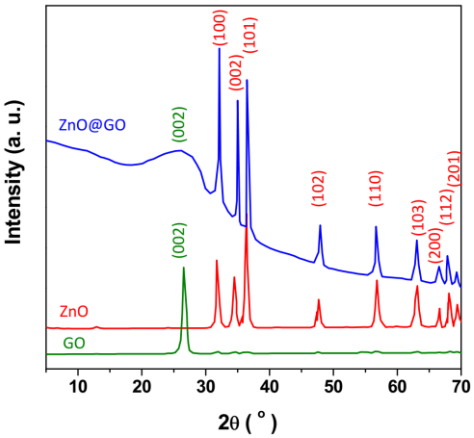

Figure 1. XRD patterns of powders of GO, ZnO and ZnO@GO nanocomposite.

Figure 2 shows SEM pictures of the morphology of GO, ZnO, and ZnO@GO nanocomposite modified SPE. As shown in Figure 2a, the SEM of GO reveals a rough and wrinkled surface with a wavy, folded structure and thin layers. The SEM picture of ZnO in Figure 2b shows an integrated structure made up of hexagonal nanorods. With an average size of 80 nm, ZnO nanorods have a comparatively high surface density. The SEM image of the ZnO@GO nanocomposite shows that ZnO nanorods with an average size of 80 nm are uniformly distributed on the surface of GO nanosheets, increasing the active sites in the modified electrode surface and increasing the effective surface area by avoiding GO nanosheet stacking and preventing ZnO agglomeration [45, 46]. The stacked GO nanosheets enwrap ZnO nanorods, signifying the production of a sandwich-like nanocomposite structure.

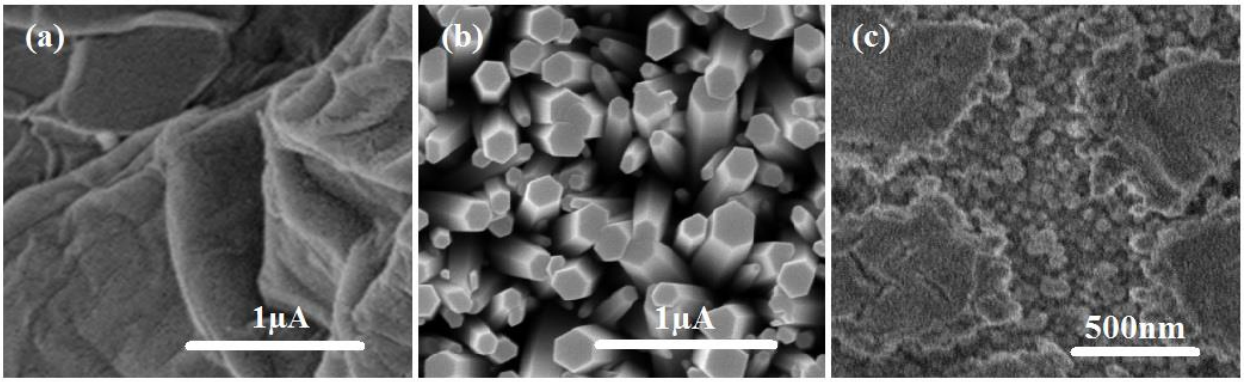

Figure 2. SEM images of (a) GO/SPE, (b) ZnO/SPE and (c) ZnO@GO/SPE.

3.2. Electrochemical studies

Figure 3 shows the DPV responses of bare SPE, GO, ZnO, and ZnO@GO nanocomposite modified SPE in 0.1 M PBS (pH 7.0) containing 30 M DEX with a scanning rate of 10 mV/s in the potential window from -1.2 V to -0.6 V in 0.1 M PBS (pH 7.0) containing 30 M DEX. The DPV curves of unmodifeid SPE do not have a recognizable peak, as shown. Meanwhile, anodic peaks at potentials

of -0.94 V, -0.95 V, and -0.93 V are observed in ZnO, GO, and ZnO@GO nanocomposite modified SPE, showing DEX reduction via the ketone groups at positions C-3 and C-20, which are possible locations for the reduction reaction [47, 48]. ZnO@GO/SPE has a lower anodic peak, and its current is approximately 2-fold and 3-fold higher than GO/SPE and ZnO/SPE, respectively. Because of the simultaneous existence of ZnO nanorods and GO nanosheets in sandwich-like ZnO@GO nanocomposites, which can avoid the agglomeration of GO nanosheets and ZnO nanorods, the ZnO@GO/SPE exhibits significant catalytic attraction in the DEX reductive process [49, 50]. As a result, the two-dimensional morphology of GO nanosheets and ZnO nanorods can improve the effective surface area at the same time [51, 52]. In addition, the oxygen-containing groups induce high catalytic activity for some reactions [53, 54]. In GO electrochemistry, the dominance of edge planes with defectivd sites such as surface functionalities, vacancies, and substrate-induced interactions provides the local density of states available for electron transfer at basal planes and nanosheet edges, and heterogeneous electron transfer occurs far more quickly at the edges of each GO nanosheet [55, 56]. As a result, the ZnO@GO nanocomposites have a large available specific surface area for analyte adsorption in the electrolyte, which improves charge transfer between the electrode and the analyte [57-59]. According to SEM data, enwrapping ZnO nanorods inside GO nanosheets precludes GO nanosheet self-aggregation and the formation of hot spots as strong electroactive sites on the electrode surface [60, 61].

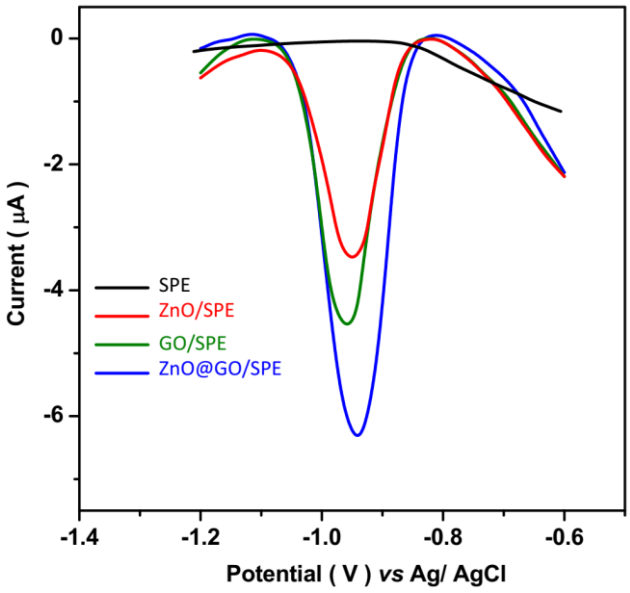

Figure 3. DPV responses of bare SPE, GO/SPE, ZnO/SPE and ZnO@GO/SPE in 0.1 M PBS (pH 7.0) containing 30 µM DEX *with* a scanning rate of 10 mV/s in the potential window from -1.2 V to -0.6 V.

Figure 4 shows the results of a study of the stability of the electrochemical response of GO, ZnO, and ZnO@GO nanocomposite modified SPE in 0.1 M PBS (pH 7.0) containing 30 M DEX with a scanning rate of 10 mV/s in the potential window from -1.2 V to -0.6 V in 0.1 M PBS (pH 7.0)

containing 30 M DEX with a scanning rate of 10 mV/s in When the current peak of ZnO/SPE, GO/SPE, and ZnO@GO/SPE is compared to the second and 75th recorded DPV curves, the current peak of ZnO/SPE, GO/SPE, and ZnO@GO/SPE drops by 7%, 10%, and 4%, respectively. The electrochemical response of ZnO@GO/SPE is determined to be the most stable because the structure of ZnO nanosheets can be maintained due to the flexibility and lubricity of GO [51]. The strong hydrogen bonding interaction between ZnO and GO, as well as the incorporation of ZnO nanorods, increases not only the exfoliation but also the uniform dispersion of GO nanosheets in nanocomposites [62, 63]. Therefore, ZnO@GO/SPE was chosen as a preferred catalyst for further electrochemical measurements of DEX sensing.

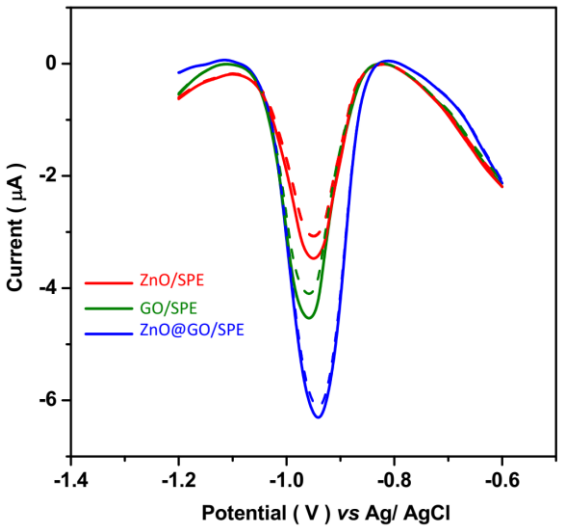

Figure 4. The second (solid line) and 75th (dashed line) recorded DPV response of GO/SPE, ZnO/SPE and ZnO@GO/SPE in 0.1 M PBS (pH 7.0) containing 30 µM DEX *with* a scanning rate of 10 mV/s in the potential window from 1.2 V to -0.6 V.

Figure 5 shows the amperomertic response and calibration plot of ZnO@GO/SPE after adding 10 µM DEX solution to 0.1 M PBS (pH 7.0) at -0.93 V. With a correlation coefficient of 0.99975, the amperomertic response of ZnO@GO/SPE grows linearly with each addition of 10 µM DEX solution in the range of 10 to 200 mM. The following is an ideal linear relationship between amperomertic currents and DEX concentrations [64]:

$$I\ (\mu A) = 0.20211 \times (\mu A/\mu M) + 0.01443 \qquad (1)$$

Where x represents the DEX concentration. The DEX amperomertic sensor's sensitivity and limit of detection (LOD) were determined to be 0.20211 µA/µM and 12 nM, respectively. These findings are compared to DEX electrochemical sensors reported in the literature (Table 1), and the results show that the developed DEX sensor using ZnO@GO/SPE has a comparable or even better sensing performance than other reported DEX sensors, which can be attributed to good stability and a large accessible specific surface area for analyte adsorption from the electrolyte, as well as improved charge transfer between the electrode and the analyte of ZnO@GO nanocomposite [65-67].

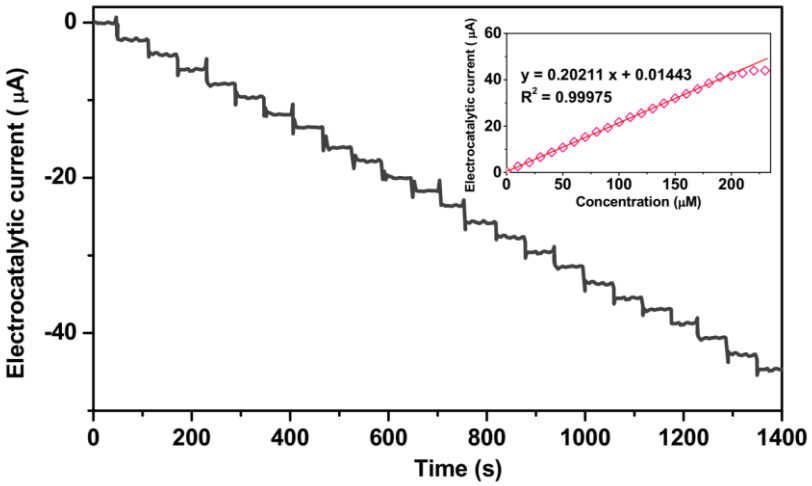

Figure 5. ZnO@GO/SPE amperomertic response and calibration plot after adding 10 μM DEX solution into 0.1 M PBS (pH 7.0) *at* potential of -0.93 V.

Table 1. Performance of DEX electrochemical sensors reported in literatures and developed DEX sensor using ZnO@GO/SPE.

Electrode	**Technique**	**LOD (nM)**	**Linear range (μM)**	**Ref.**
ZnO@GO/SPE	Amperomertry	12	10 –200	This work
β-cyclodextrin/CPE	DPV	1500	0.41–20	[31]
C_{60}/EPPGE	OSWV	55	0.05–100	[20]
MWCNTs/PE	SWV	90	0.15-100	[32]
Fe_3O_4/ polyaniline–Cu^{II}/CILE	DPV	3.0	0.05–30	[33]
amalgam film silver based electrode	CV	1.6	0.0025–0.225	[34]
Aptamer/Au electrode	EIS	2.12	0.0025–0.1	[35]

CPE: carbon paste electrode; EPPGE: edge plane pyrolytic graphite electrode; OSWV: Osteryoung square wave voltammetry; PE: pencil electrode; SWV: square wave voltammetry; CILE: carbon ionic liquid electrode; CV: cyclic voltammetry, EIS: Electrochemical impedance spectroscopy

The impact of potentially interfering chemicals on DEX detection was looked at. Figure 6 shows the results of amperomertic currents of ZnO@GO/SPE at -0.93 V in 0.1 M PBS (pH 7.0) under the addition of DEX and 5-fold excesses of interfering compounds, demonstrating that the amperomertic sensor response to 10 μM DEX solution is remarkably greater than that of interfering substances, and that the amperomertic signal of DEX at -0.93 V to the addition of 5-fold excesses shows no significant change. These results show that the proposed sensor can detect DEX in pharmaceutical and biological fluid samples with a high degree of selectivity.

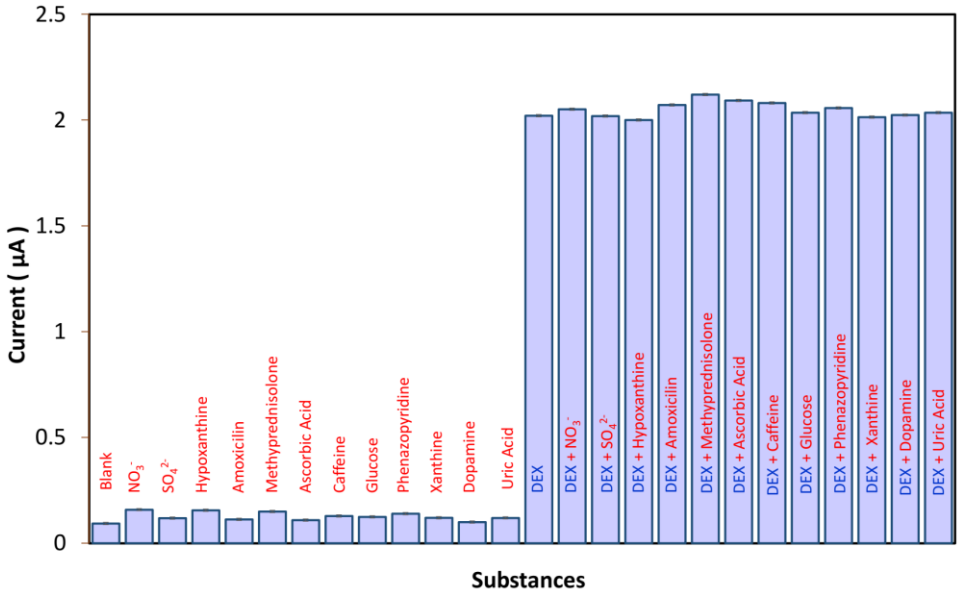

Figure 6. The results of amperomertic currents of ZnO@GO/SPE at -0.93 V under successive additions of 10 µM DEX and 5-fold excesses interfering compounds 0.1 M PBS (pH 7.0) (Blank sample is referred to the 0.1 M PBS without any analyte)

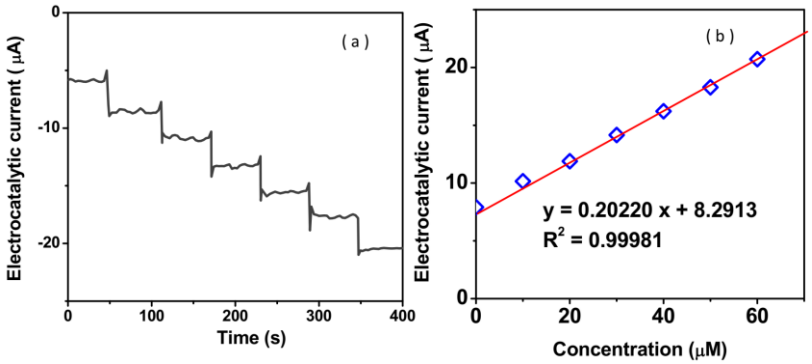

Figure 7. (a) Amperomertic response and (b) calibration plot of ZnO@GO/SPE in prepared actual sample under successive additions of 10 µM DEX at -0.93 V

The practical potential of ZnO@GO/SPE for determining DEX level in dexamethasone injection was investigated. Figure 7 shows the obtained amperomertic response and calibration curve in a prepared actual sample after 10 µM DEX was added at -0.93 V in steps. The DEX content in pharmaceutical dexamethasone injection is 41.0 µM, according to the produced calibration plot. This is consistent with the injection's indicated value. Table 2 shows the proper recovery (96.50% to 99.16%) and RSD (3.33% to 4.35%) values for practical analyses in clinical and pharmaceutical samples, indicating appropriate validity and accuracy.

Table 2. Analytical analyses of ZnO@GO/SPE for determination DEX in prepared actual samples of dexamethasone injection.

Added (μM)	**Found (μM)**	**Recovery (%)**	**RSD (%)**
10.0	9.9	99.00	4.20
20.0	19.3	96.50	3.71
30.0	29.7	99.00	3.65
40.0	39.6	99.00	4.35
50.0	49.4	98.80	3.33
60.0	59.5	99.16	3.74

4. CONCLUSION

The goal of this project was to create ZnO@GO/SPE and conduct electrochemical tests to determine DEX in pharmaceutical samples. A simple chemical process was used to make the ZnO@GO nanocomposite. The results showed that the hexagonal crystal structure of GO nanosheets and hexagonal wurtzite ZnO nanorods were successfully combined into a sandwich-like ZnO@GO nanocomposite structure. According to electrochemical tests, ZnO@GO/SPE is a more selective, stable, and sensitive DEX sensor than ZnO/SPE and GO/SPE. The ZnO@GO/SPE had a linear range of 10 to 200 μM, a sensitivity of 0.20211 μA/μM, and a limit of detection of 12 nM, indicating that it had similar or even superior sensing capability as other DEX sensors reported in the literature. The practical capability to ZnO@GO/SPE was investigated for determining DEX level in dexamethasone injection, and the results revealed appropriate recovery (96.50–99.16%) and RSD (3.33–4.35%) values, indicating appropriate validity and accuracy for practical analyses in clinical and pharmaceutical samples.

References

1. A.K. Aljarah, I.H. Hameed and M.Y. Hadi, *Indian Journal of Forensic Medicine & Toxicology*, 13 (2019) 1.
2. T. Gao, C. Li, Y. Zhang, M. Yang, D. Jia, T. Jin, Y. Hou and R. Li, *Tribology International*, 131 (2019) 51.
3. L. Jiang, Y. Wang, X. Wang, F. Ning, S. Wen, Y. Zhou, S. Chen, A. Betts, S. Jerrams and F.-L. Zhou, *Composites Part A: Applied Science and Manufacturing*, 147 (2021) 106461.
4. M. Vormehr, S. Lehar, L.M. Kranz, S. Tahtinen, Y. Oei, V. Javinal, L. Delamarre, K.C. Walzer, M. Diken and S. Kreiter, *Oncoimmunology*, 9 (2020) 1758004.
5. H. Maleh, M. Alizadeh, F. Karimi, M. Baghayeri, L. Fu, J. Rouhi, C. Karaman, O. Karaman and R. Boukherroub, *Chemosphere*, (2021) 132928.
6. R. Rahmi, S. Lubis, N. Az-Zahra, K. Puspita and M. Iqhrammullah, *International Journal of Engineering*, 34 (2021) 1827.
7. C. Liu and J. Rouhi, *RSC Advances*, 11 (2021) 9933.
8. A.S. Chouhan, B. Parihar, B. Rathod and R. Prajapat, *Systematic Reviews in Pharmacy*, 12 (2021) 3772.

9. M. Yang, C. Li, Y. Zhang, D. Jia, R. Li, Y. Hou, H. Cao and J. Wang, *Ceramics International*, 45 (2019) 14908.
10. X. Hu, P. Zhang, D. Wang, J. Jiang, X. Chen, Y. Liu, Z. Zhang, B.Z. Tang and P. Li, *Biosensors and Bioelectronics*, 182 (2021) 113188.
11. W.-F. Lai, R. Tang and W.-T. Wong, *Pharmaceutics*, 12 (2020) 725.
12. J. Yan, Y. Yao, S. Yan, R. Gao, W. Lu and W. He, *Nano Letters*, 20 (2020) 5844.
13. T. Li, D. Shang, S. Gao, B. Wang, H. Kong, G. Yang, W. Shu, P. Xu and G. Wei, *Biosensors*, 12 (2022) 314.
14. M.P. Mead, J.P. Gumucio, T.M. Awan, C.L. Mendias and K.B. Sugg, *Translational sports medicine*, 1 (2018) 5.
15. Z. Zhang, P. Ma, R. Ahmed, J. Wang, D. Akin, F. Soto, B.F. Liu, P. Li and U. Demirci, *Advanced Materials*, 34 (2022) 2103646.
16. D.S. Samuel and S.P. Priyadarshoni, *Drug Invention Today*, 11 (2019) 1.
17. Z. Zhuo, Y. Wan, D. Guan, S. Ni, L. Wang, Z. Zhang, J. Liu, C. Liang, Y. Yu and A. Lu, *Advanced Science*, 7 (2020) 1903451.
18. T.K. Karatt, R. Sayed, J. Nalakath, Z. Perwad, P.H. Albert and K.K. Abdul Khader, *Steroids*, 140 (2018) 77.
19. Z. Li, M. Teng, R. Yang, F. Lin, Y. Fu, W. Lin, J. Zheng, X. Zhong, X. Chen and B. Yang, *Sensors and Actuators B: Chemical*, 361 (2022) 131691.
20. R.N. Goyal, V.K. Gupta and S. Chatterjee, *Biosensors and Bioelectronics*, 24 (2009) 1649.
21. E. Darezereshki, A. Behrad Vakylabad and M. Yousefi, *International Journal of Engineering*, 34 (2021) 1888.
22. M. Liu, C. Li, Y. Zhang, Q. An, M. Yang, T. Gao, C. Mao, B. Liu, H. Cao and X. Xu, *Frontiers of Mechanical Engineering*, 16 (2021) 649.
23. H. Karimi-Maleh, R. Darabi, M. Shabani-Nooshabadi, M. Baghayeri, F. Karimi, J. Rouhi, M. Alizadeh, O. Karaman, Y. Vasseghian and C. Karaman, *Food and Chemical Toxicology*, 162 (2022) 112907.
24. L. Nan, C. Yalan, L. Jixiang, O. Dujuan, D. Wenhui, J. Rouhi and M. Mustapha, *RSC Advances*, 10 (2020) 27923.
25. V. Baeyens, E. Varesio, J.-L. Veuthey and R. Gurny, *Journal of Chromatography B: Biomedical Sciences and Applications*, 692 (1997) 222.
26. H.M. Lotfy, Y.M. Fayez, S.M. Tawakkol, N.M. Fahmy and M.A.E.-A. Shehata, *Analytical Chemistry Letters*, 7 (2017) 30.
27. O. Huetos, M. Ramos, M.M. de Pozuelo, T.B. Reuvers and M. San Andrés, *Analyst*, 124 (1999) 1583.
28. O.H. Hidalgo, M.J. López, E.A. Carazo, M.S.A. Larrea and T.B. Reuvers, *Journal of Chromatography B*, 788 (2003) 137.
29. J. English, J. Chakraborty, V. Marks and A. Parke, *European journal of clinical pharmacology*, 9 (1975) 239.
30. M.a.S. Collado, J.C. Robles, M. De Zan, M.a.S. Cámara, V.c.E. Mantovani and H.C. Goicoechea, *International journal of pharmaceutics*, 229 (2001) 205.
31. K. Balaji, G.R. Reddy, T.M. Reddy and S.J. Reddy, *African Journal of Pharmacy and Pharmacology*, 2 (2008) 157.
32. B. Rezaei, S. Zare and A.A. Ensafi, *Journal of the Brazilian Chemical Society*, 22 (2011) 897.
33. A. Fatahi, R. Malakooti and M. Shahlaei, *RSC Advances*, 7 (2017) 11322.
34. J. Smajdor, R. Piech and B. Paczosa-Bator, *Journal of Electroanalytical Chemistry*, 809 (2018) 147.
35. S. Mehennaoui, S. Poorahong, G.C. Jimenez and M. Siaj, *Scientific Reports*, 9 (2019) 6600.
36. Z. Guo and H. Fan, *International Journal of Electrochemical Science*, 16 (2021) 211125.

37. Y. Chen, K. He, F. Sun, D. Wei and H. Li, *International Journal of Electrochemical Science*, 16 (2021) 210321.
38. F. Qin, T. Hu, L. You, W. Chen, D. Jia, N. Hu and W. Qi, *International Journal of Electrochemical Science*, 17 (2022) 220426.
39. E. Salih, M. Mekawy, R.Y.A. Hassan and I.M. El-Sherbiny, *Journal of Nanostructure in Chemistry*, 6 (2016) 137.
40. P. Dash, T. Dash, T.K. Rout, A.K. Sahu, S.K. Biswal and B.K. Mishra, *RSC advances*, 6 (2016) 12657.
41. R. Savari, J. Rouhi, O. Fakhar, S. Kakooei, D. Pourzadeh, O. Jahanbakhsh and S. Shojaei, *Ceramics International*, 47 (2021) 31927.
42. J. Rouhi, H.K. Malayeri, S. Kakooei, R. Karimzadeh, S. Alrokayan, H. Khan and M.R. Mahmood, *International Journal of Electrochemical Science*, 13 (2018) 9742.
43. H. Savaloni and R. Savari, *Materials Chemistry and Physics*, 214 (2018) 402.
44. T. Gao, Y. Zhang, C. Li, Y. Wang, Q. An, B. Liu, Z. Said and S. Sharma, *Scientific reports*, 11 (2021) 1.
45. A. Abdul Rahman–Al Ezzi, *International Journal of Engineering*, 33 (2020) 2120.
46. W.-F. Lai, D. Gui, M. Wong, A. Döring, A.L. Rogach, T. He and W.-T. Wong, *Journal of Drug Delivery Science and Technology*, 63 (2021) 102428.
47. S. Alimohammadi, M.A. Kiani, M. Imani, H. Rafii-Tabar and P. Sasanpour, *Scientific Reports*, 9 (2019) 11775.
48. Z. Said, S. Arora, S. Farooq, L.S. Sundar, C. Li and A. Allouhi, *Solar Energy Materials and Solar Cells*, 236 (2022) 111504.
49. Y. Qi, C. Zhang, S. Liu, Y. Zong and Y. Men, *Journal of Materials Research*, 33 (2018) 1506.
50. H. Karimi-Maleh, C. Karaman, O. Karaman, F. Karimi, Y. Vasseghian, L. Fu, M. Baghayeri, J. Rouhi, P. Senthil Kumar and P.-L. Show, *Journal of Nanostructure in Chemistry*, (2022) 1.
51. P. Wang, D. Wang, M. Zhang, Y. Zhu, Y. Xu, X. Ma and X. Wang, *Sensors and Actuators B: Chemical*, 230 (2016) 477.
52. A. Jahanbakhsh, M. Hosseini, M. Jahanshahi and A. Amiri, *International Journal of Engineering*, 35 (2022) 988.
53. F. Yang, X. Ma, W.-B. Cai, P. Song and W. Xu, *Journal of the American Chemical Society*, 141 (2019) 20451.
54. A. Ejaz, H. Babar, H.M. Ali, F. Jamil, M.M. Janjua, I.R. Fattah, Z. Said and C. Li, *Sustainable Energy Technologies and Assessments*, 46 (2021) 101199.
55. K.R. Ratinac, W. Yang, J.J. Gooding, P. Thordarson and F. Braet, *Electroanalysis*, 23 (2011) 803.
56. S. Changaei, J. Zamir-Anvari, N.-S. Heydari, S.G. Zamharir, M. Arshadi, B. Bahrami, J. Rouhi and R. Karimzadeh, *Journal of Electronic Materials*, 48 (2019) 6216.
57. W. Huang, Y. Xu and Y. Sun, *Frontiers in Chemistry*, 10 (2022) 1.
58. R. Hassanzadeh, A. Siabi-Garjan, H. Savaloni and R. Savari, *Materials Research Express*, 6 (2019)
59. H. Savaloni, R. Savari and S. Abbasi, *Current Applied Physics*, 18 (2018)
60. M. Zarrabi, M. Haghighi and R. Alizadeh, *Ultrasonics Sonochemistry*, 48 (2018) 370.
61. X. Xue, H. Liu, S. Wang, Y. Hu, B. Huang, M. Li, J. Gao, X. Wang and J. Su, *Composites Part B: Engineering*, 237 (2022) 109855.
62. Y. Lu, X. Xie, W.-y. Wang, X.-d. Qi, Y.-z. Lei, J.-h. Yang and Y. Wang, *Composites Part A: Applied Science and Manufacturing*, 124 (2019) 105489.
63. D. Shi, Y. Chen, Z. Li, S. Dong, L. Li, M. Hou, H. Liu, S. Zhao, X. Chen and C.P. Wong, *Small Methods*, (2022) 2200329.
64. Q.-M. Xiong, Z. Chen, J.-T. Huang, M. Zhang, H. Song, X.-F. Hou, X.-B. Li and Z.-J. Feng, *Rare metals*, 39 (2020) 589.

65. Z. Savari, S. Soltanian, A. Noorbakhsh, A. Salimi, M. Najafi and P. Servati, *Sensors and Actuators B: Chemical*, 176 (2013) 335.
66. H. Karimi-Maleh, H. Beitollahi, P.S. Kumar, S. Tajik, P.M. Jahani, F. Karimi, C. Karaman, Y. Vasseghian, M. Baghayeri and J. Rouhi, *Food and Chemical Toxicology*, (2022) 112961.
67. G. Wang, D. Liu, S. Fan, Z. Li and J. Su, *Nanotechnology*, 32 (2021) 215202.